The Electronic Structures and Formation Mechanisms of the Single-Walled BN Nanotube with Small Diameter

Hua Xu, Jing Ma,* Xin Chen, Zheng Hu,* Kaifu Huo, and Yi Chen

Key Lab of Mesoscopic Chemistry and Jiangsu Provincial Lab for Nano Technology, Institute of Theoretical and Computational Chemistry, Department of Chemistry, Nanjing University, Nanjing 210093 China

Received: June 27, 2003; In Final Form: November 10, 2003

A possible smallest single-walled BN nanotube with the diameter of 0.4 nm is proposed. The studied nanotube is of armchair (3,3) and thought to be associated with the BN fullerene, $B_{12}N_{12}$. We have applied the ab initio MP2/6-31G//HF/6-31G method to investigate the growth mechanisms of this nanotube from $B_{12}N_{12}$. Our results show that a $B_{12}N_{12}$ fullerene may react with B_2H_6 and NH_3 to form an armchair (3,3) tubular structure under certain experimental conditions such as high temperature. The armchair (3,3) tube can continuously incorporate B and N atoms to grow and can also disassociate H_2 to close into a half-$B_{12}N_{12}$ cap. The growth of the tube is predicted to be favorable to the capping of the tube in an atmosphere with B_2H_6 and NH_3 in it. And the cap of the tube is relatively easier to be opened by H_2 or B_2H_6 and NH_3 to convert to a growing open-ended tube.

1. Introduction

The study on the synthesis and properties of one-dimensional nanostructures such as nanotubes (NTs) and nanowires (NWs) has gained considerable attention because of their importance in both mesoscopic research and the development of nanodevices.[1,2] Since the discovery of C_{60} and carbon nanotubes (CNTs), a parallelism between small stable fullerenes and obtained nanotubes has been recognized, e.g., the "smallest" CNTs with the diameters of 0.7,[3] 0.5,[4] and 0.4 nm[5−7] were associated with C_{60}, C_{36}, and C_{20}, respectively. This consistency is expected to be also valid for the boron nitride (BN) system due to the similarity between hexagonal BN and graphite in the bond length, the long-order parameters, and the lattice constants.[8] Among BN fullerenes, $B_{12}N_{12}$ and $B_{16}N_{16}$ are the smallest anomalously stable clusters with T symmetry[9−12] and also the smallest reported fullerenes.[13,14] These two fullerenes are considered to be associated with the armchair (3,3) and zigzag (6,0) BN nanotubes, respectively (Chart 1). Considering the anomalous stabilities of the $B_{12}N_{12}$ and $B_{16}N_{16}$ fullerenes, two corresponding tubular structures are expected to be attainable. The zigzag (6,0) BN tube with a diameter of 0.5 nm has been reported by E. Bengu and L. D. Marks.[15]

Until now, however, no report has appeared concerning the preparation and theoretical calculations of the armchair (3,3) BN tube, which is parallel to be the smallest carbon nanotube with the diameter of 0.4 nm. By analogy to the smallest CNTs,[16] some unusual properties of this BN tube due to the largely increased curvature and strain energy could be expected. Therefore, in this theoretical work, we aim to understand properties of electronic structures of armchair (3,3) BN tube and its possible growth mechanisms starting from $B_{12}N_{12}$.

Our calculations show that the armchair (3,3) BN tube has a very close thermodynamic stability to and greater kinetic stability than the known zigzag (6,0) one. Therefore, it is quite reasonable to anticipate that the armchair (3,3) tube can be prepared just as the zigzag (6,0) one. Then, the possible formation mechanisms of the armchair (3,3) tube from $B_{12}N_{12}$ and the further growth process are also investigated in the atmosphere with B_2H_6 and NH_3 (Scheme 1). The possibility of the formation and the growth of the armchair (3,3) tube in experimental conditions is suggested by our calculations.

CHART 1. BN Fullerenes vs Nanotubes[a]

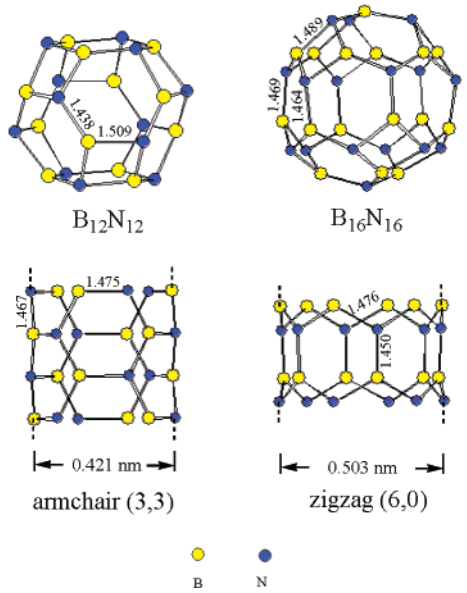

[a] The geometries of BN tubes are estimated from results of HF/3-21G optimizations on $H_6(B_6N_6)_{17}H_6$.

2. Computational Details

All calculations have been performed with the Gaussian 98 package[17] on the SGI 3800 workstation of Nanjing University.

Validations. As pointed out by Zhang et al. from their extensive studies,[18] it is very important to select the suitable basis sets that can maintain the accuracy of the result within the available computational resources. Therefore, we first use $B_{12}N_{12}$ as a model substance to test the influence of methods and basis sets on the optimized geometries (Table 1). From Table 1, we can see that calculations using various methods and basis sets yield almost identical predictions on the B−N

* Authors to whom correspondence may be addressed. E-mail: zhenghu@nju.edu.cn (Z.H.); majing@netra.nju.edu.cn (J.M.).

10.1021/jp035845m CCC: $27.50
Published on Web 03/09/2004

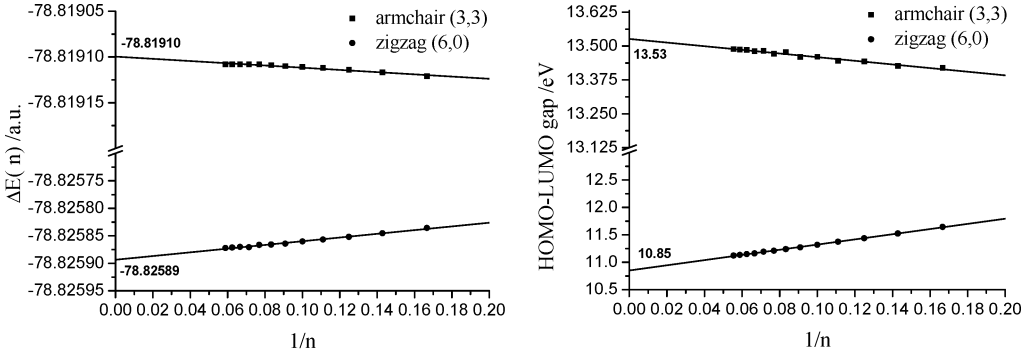

Figure 1. (a) $\Delta E(n)$ and (b) HOMO−LUMO gap as functions of the reciprocal of the tubular length n.

SCHEME 1. Formation and Growth Mechanisms of the Armchair (3,3) BN Tube

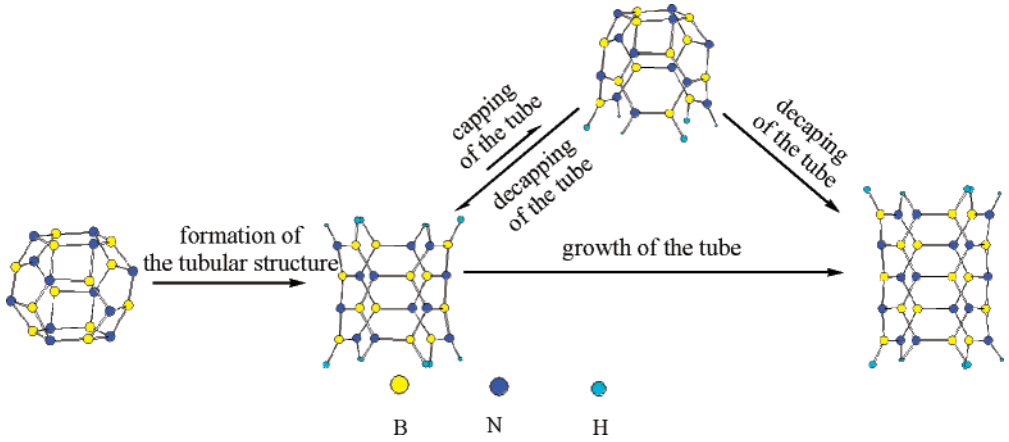

TABLE 1: Optimized Geometries of $B_{12}N_{12}$ Fullerene by Various Methods and Basis Sets

$B_{12}N_{12}$	$R_{B-N}(6-6)^a$ (Å)	$R_{B-N}(4-6)^b$ (Å)	d^c (nm)
HF/3-21G	1.438	1.509	0.444
HF/6-31G	1.430	1.497	0.441
HF/6-31G(d)	1.433	1.475	0.434
B3LYP/3-21G	1.442	1.516	0.445
B3LYP/6-31G	1.435	1.505	0.442
B3LYP/6-31G(d)	1.439	1.486	0.437
MP2/3-21G	1.454	1.532	0.449
MP2/6-31G	1.449	1.524	0.447
MP2/6-31G(d)	1.443	1.488	0.437

[a] $R_{B-N}(6-6)$ is the bond length of the B−N bonds shared by two hexagons. [b] $R_{B-N}(4-6)$ is the bond length of the B−N bonds shared by a square and a hexagon. [c] d is the fullerene diameters along C_3 axes.

bond lengths and diameter of $B_{12}N_{12}$ fullerene. Thus, to save the computational cost, the Hartree−Fock (HF) method with the 6-31G basis set is employed in the geometry optimization for the fullerenes and tubes.

On the other hand, since we are interested in the formation and growing mechanisms of the BN nanotube, the influence of basis sets on the relative energies of reactants, transition states, and products is then validated by the pathways in the formation reaction of the tubular structure from $B_{12}N_{12}$ fullerene (i.e., the first step in Scheme 1). Both 6-31G and 6-31G(d) basis sets are employed in the MP2 calculations of all species (systems **1**−**12** in Figure 2) along reaction pathways with the detailed results given in the Supporting Information. The differences in the activation energies and reaction energies caused by these two basis sets are found to be even for all steps. The global shapes of the potential energy profiles are nearly not affected by the selection of basis sets. Here, the influence of basis sets is briefly illustrated by a process of the addition of NH_3 on $B_{12}N_{12}$ (**1** in Figure 2) to form a fullerene−NH_3 complex (**7** in Figure 2). For this step, the calculations by using the 6-31G and 6-31G(d) basis sets give the association energies of 47.71 and 44.33 kcal/mol, respectively. So, MP2/6-31G is employed in this work to calculate energies of reactants, intermediates, transition states, and products, reaching a compromise between the computational expense and accuracy. In addition, the economic basis set proposed by Zhang et al.[18] is also a good choice for our future studies on large systems. All the intermediates and transition states are checked by frequency calculations.

Nanotube Models. We select tube models of $H_6(B_6N_6)_nH_6$, $n = 6-17$ to study electronic structures of BN single-walled tubes with the relative length of the tube defined as n. To reduce the computational load, a 3-21G basis set is used in the geometry optimization for these long BN nanotubes ($H_6(B_6N_6)_nH_6$, $n = 6-17$). Both ends of the BN tube are saturated by hydrogen atoms. Reasonable predictions of the geometry and stability of BN tubes can be anticipated by limiting our attention to the electronic structure at the middle part of the studied BN tubes and by comparing the change in ground-state energy per (BN) unit, i.e., the $\Delta E(n)$ to exclude boundary effects. The definition of $\Delta E(n)$ is given as follows

$$\Delta E(n) = [E(H_6(B_6N_6)_{n+1}H_6) - E(H_6(B_6N_6)_nH_6)]/6 \quad (1)$$

3. Results and Discussion

3.1. Electronic Structures of Nanotubes and Their Associated Fullerenes. We have applied the HF method with a 3-21G basis set to study electronic structures of the armchair (3,3) and zigzag (6,0) single-walled tubes with the increasing tube length, i.e., $H_6(B_6N_6)_nH_6$, $n = 6-17$. On the basis of these results, properties of infinite tubes are then reasonably extrapo-

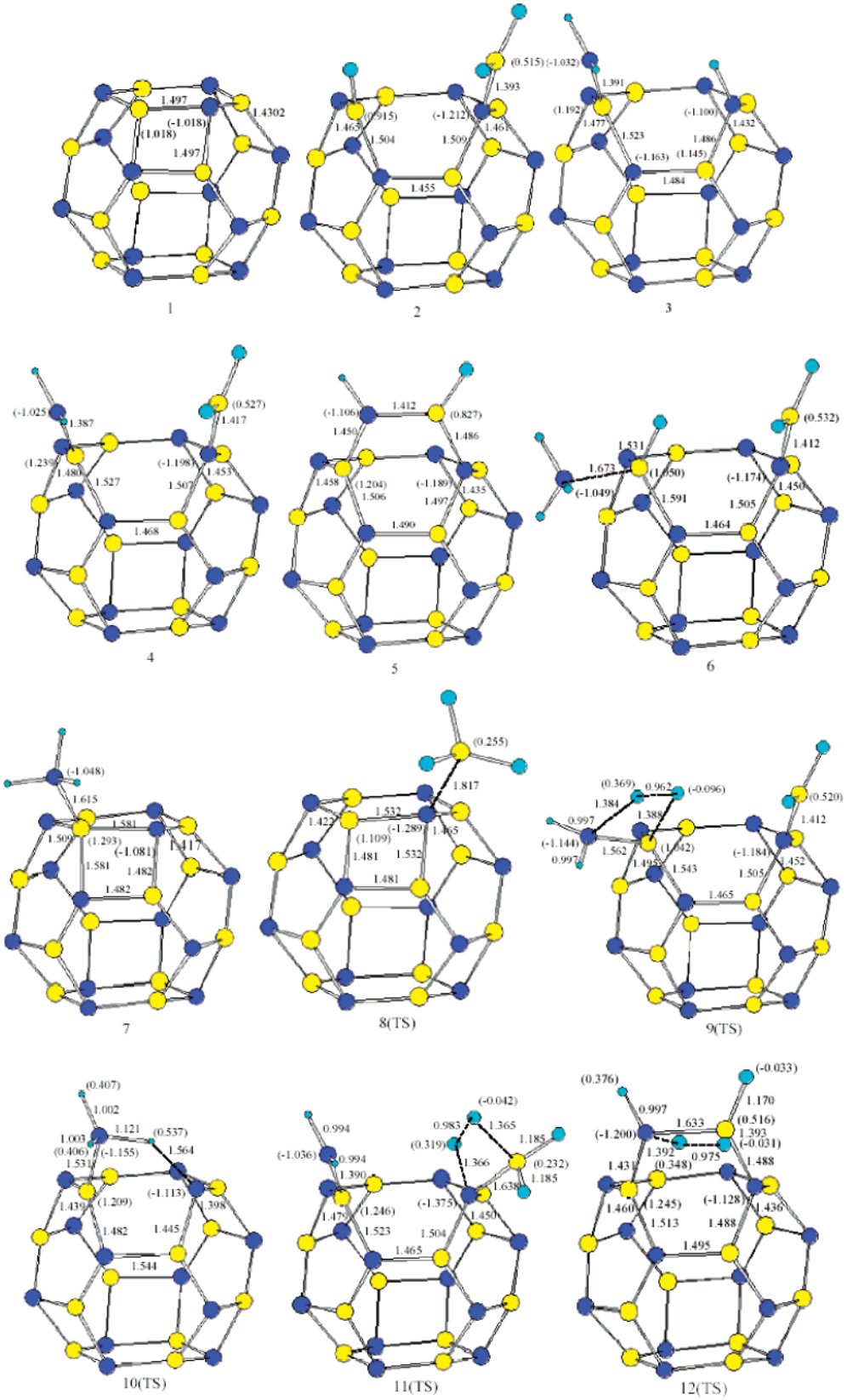

Figure 2. The optimized structures of all reactants, intermediates, transition states, and products during formation processes of the armchair (3,3) tubular structure at the HF/6-31G level.

lated when $1/n$ approaches zero. The relationship between these two kinds of single-walled tubes and their associated fullerenes, $B_{12}N_{12}$, and $B_{16}N_{16}$, are also addressed in the following.

Geometry. When the studied single-walled tubes, $H_6(B_6N_6)_nH_6$, are long enough, i.e., $n > 15$, geometrical parameters of the central parts of long armchair (3,3) and zigzag (6,0) tubes become convergent to constant values. So, we take those converged structural parameters of these two tubes (shown in Chart 1) as approximate properties of real infinite armchair (3,3) and zigzag (6,0) tubes, which are compared in Table 2 with those of the corresponding fullerenes. The diameter of the armchair (3,3) tube is 0.421 nm, close to that of $B_{12}N_{12}$ fullerene,

TABLE 2: Electronic Structures of the Armchair (3,3) and Zigzag (6,0) BN Single-Walled Nanotubes and $B_{12}N_{12}$, and $B_{16}N_{16}$ Fullerenes

	symmetry	d^a (nm)	$E/N_b{}^b$ (kcal/mol)	HOMO−LUMO gap (eV)
armchair (3,3) tube	S_6	0.421	0.0	13.53
zigzag (6,0) tube	C_{6v}	0.503	−4.2608	10.85
$B_{12}N_{12}$ fullerene	T_h	0.444	28.8826	13.50
$B_{16}N_{16}$ fullerene	T_d	0.517	20.1966	13.29

[a] The diameters of the BN fullerenes are along C_3 axes. The structural parameters of the central parts of long armchair (3,3) and zigzag (6,0) tubes, $H_6(B_6N_6)_nH_6$ ($n > 15$), are very close to and considered to be the parameters of their infinite tubes. [b] E/N_b is the relative ground-state energy per (BN) unit. The ground-state energy per (BN) unit of the infinite armchair (3,3) tube, −78.81910 au, is taken as the zero for comparing the relative energies between infinite armchair (3,3) and zigzag (6,0) BN single-walled nanotubes and $B_{12}N_{12}$ and $B_{16}N_{16}$ fullerenes.

0.444 nm. The zigzag (6,0) tube has a slightly larger diameter of 0.503 nm, which is also close to that of $B_{16}N_{16}$ fullerene, 0.517 nm. Furthermore, the optimized configurations (Chart 1) show that the central parts of the $B_{12}N_{12}$ and $B_{16}N_{16}$ fullerenes are of armchair (3,3) and zigzag (6,0) structures, respectively. Thus, the $B_{12}N_{12}$ and $B_{16}N_{16}$ fullerenes are associated with and able to cap the armchair (3,3) and zigzag (6,0) BN tubular structures.

B−N bonds are elongated in both armchair (3,3) and zigzag (6,0) tubular configurations due to the strain effect. We find in Chart 1 that the elongation of bond length takes place in different degrees in these two tubular structures. For the armchair (3,3) tubular structure, the B−N bond alternates between 1.467 and 1.475 Å with a small bond length alternation of 0.008 Å, showing an extensive electron delocalization in this nanotube. In fact, similar small bond alternations of 0.005 Å for Al−N bonds in the armchair AlN tube and 0.072 Å for C−C bonds in an armchair carbon tube are recently reported by using HF/3-21G(d) calculations.[19] The zigzag (6,0) BN tube has relatively larger bond alternations of 0.026 Å than that of the armchair (3,3) one (0.008 Å). This is understandable, since the strain effect of the armchair (3,3) acts almost evenly on all of its bonds, while the strain effect of the zigzag (6,0) concentrates on its partial bonds. So half of the B−N bonds in the zigzag (6,0) tube are elongated negligibly and their bond lengths of 1.450 Å are close to that of bulky h-BN.

Ground-State Energy. For the tube of $H_6(B_6N_6)_nH_6$, we calculate the ground-state energies from $n = 6-17$ at their optimized geometries. As introduced in section 2, we have applied the ground-state energy per (BN) unit $\Delta E(n)$ (eq 1) to study the relative stabilities of tubular structures. Figure 1a shows the $\Delta E(n)$ as a function of the reciprocal of n, the length of the tube. When the reciprocal of n approaches zero, the $\Delta E(n)$ is approximately corresponding to the energy per (BN) unit of the infinite tube E/N_b. As shown in Figure 1a, the extrapolated energies per (BN) unit of the armchair (3,3) and zigzag (6,0) tubes are −78.81910 and −78.82589 au, respectively. Because of the larger strain effects in small cages, the energies per (BN) unit of their fullerenes, $B_{12}N_{12}$ and $B_{16}N_{16}$, are higher (−78.77307 and −78.78691 au, respectively). Taking the energy per (BN) unit of the armchair (3,3) tube as the zero for comparison, the relative energies per (BN) unit of the armchair (3,3) and zigzag (6,0) tubes, $B_{12}N_{12}$ and $B_{16}N_{16}$, are listed in Table 2. The armchair (3,3) BN tube has a comparable thermodynamic stability to the observed zigzag (6,0) BN tube, and the corresponding fullerene $B_{12}N_{12}$ also has a similar stability to $B_{16}N_{16}$, the fullerene of the zigzag (6,0). The relatively more stable zigzag (6,0) BN tube and $B_{16}N_{16}$ structures can be understood by their larger radii and hence smaller strain energies than those of the armchair (3,3) BN tube and $B_{12}N_{12}$.

HOMO−LUMO Gap. Energy gaps between the HOMOs and LUMOs of the armchair (3,3) and zigzag (6,0) tubes and their fullerenes are helpful to compare their relative kinetic stabilities, which are also given in Table 2. Figure 1b displays variations in HOMO−LUMO gaps of tubes with the reciprocal of n. Our results show that the HOMO−LUMO gaps of the infinite armchair (3,3) and zigzag (6,0) tubes are 13.53 and 10.85 eV, respectively. This indicates that the infinite armchair (3,3) tube may have a slightly greater kinetic stability than the zigzag (6,0) one. The HOMO−LUMO gap of $B_{12}N_{12}$, 13.50 eV, is very close to that of $B_{16}N_{16}$, 13.29 eV. Zhang et al.[19] have given comparable HOMO−LUMO gaps of 8.04 and 10.09 eV for the armchair carbon and AlN nanotubes, respectively (HF/3-21G-(d)).

To summarize, the armchair (3,3) BN tube has a comparable thermodynamic stability to and slightly greater kinetic stability than the zigzag (6,0) BN tube. Such a comparable stability also exists in their corresponding fullerenes, $B_{12}N_{12}$ and $B_{16}N_{16}$. Therefore, it is quite reasonable to anticipate that the armchair (3,3) may also be prepared someday, just as the zigzag (6,0), which has already been observed in E. Bengu's experiment.[15]

3.2. Growth Mechanisms of the Armchair (3,3) BN Nanotube. Starting from the $B_{12}N_{12}$ fullerene, the proposed mechanisms of the formation and further growth of the armchair (3,3) BN tube include two main processes: (1) the formation of the tubular structure and (2) the growth of the tube in the atmosphere of H_2, B_2H_6, and NH_3 (cf. Scheme 1). During the growth of the tube, it is also possible for the tube to be closed into a cap, which may compete with the tube's further growth. While the cap can be also destroyed by further additions of H_2, B_2H_6, and NH_3 and again, the tube can be converted to a growing open-ended structure. To study mechanisms of these processes, MP2/6-31G//HF/6-31G calculations have been carried out with results presented below.

The Formation of the Armchair (3,3) Tubular Structure. Because of the above-mentioned association between the armchair (3,3) BN tube and $B_{12}N_{12}$ fullerene, there is a possibility that the tube could grow from the $B_{12}N_{12}$ fullerene. In addition, some big fullerenes (such as $B_{60}N_{60}$ fullerene with squares, hexagons, and octagons)[20] have the partial $B_{12}N_{12}$ fullerene strucuture and greater thermodynamic stability than the $B_{12}N_{12}$ fullerene. The possible formation mechanism of the tubular structure from that kind of big fullerene is conceived to be similar to that growing from the $B_{12}N_{12}$ fullerene. For the sake of computational advantages, we select $B_{12}N_{12}$ fullerene (**1**) as a model reactant to investigate the formation and growth mechanisms of the armchair (3,3) BN tube.

In the $B_{12}N_{12}$ fullerene (**1**), squares are less stable and more readily to be destructed than hexagons. The opening of squares and the formation of new hexagons can initiate an armchair (3,3) tubular structure. Scheme 2 depicts the possible processes of the reaction of the $B_{12}N_{12}$ fullerene (**1**) with B_2H_6 and NH_3 to open one square and form one hexagon, which is the first step of the formation of the armchair (3,3) tubular structure. In Scheme 2, there are two possible pathways: one is the path I where reactant **1** incorporates a B atom from B_2H_6 to open a square in an intermediate **2** and subsequently incorporates a N atom from NH_3 to form a hexagon in **4** and another one is path II, involving a reaction of $B_{12}N_{12}$ fullerene (**1**) with a NH_3 molecule, giving intermediate **3** first and then with the B_2H_6 to form a hexagon.

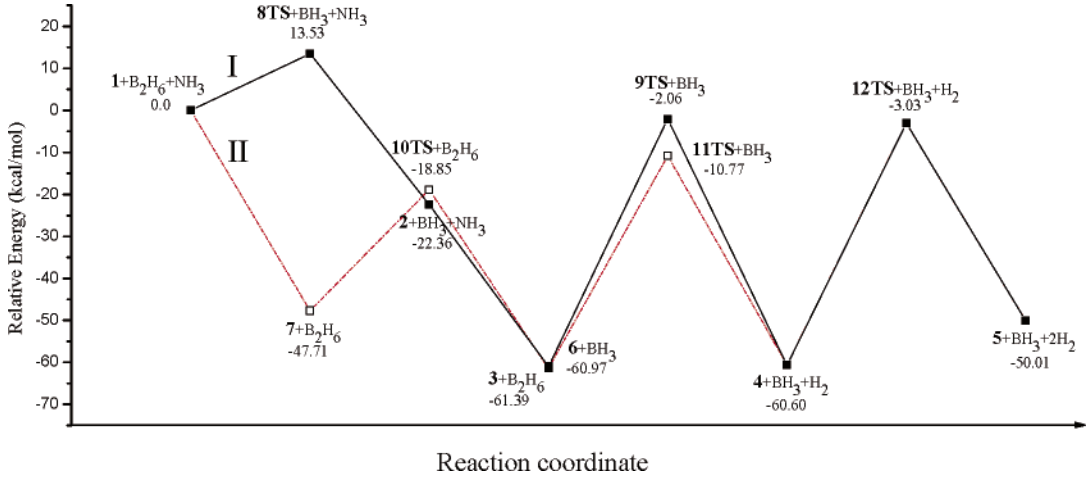

Figure 3. Potential energy profiles for the formation of the armchair (3,3) tubular structure via paths I and II (cf. Scheme 2).

SCHEME 2. Formation Paths of the Armchair (3,3) Tubular Structure

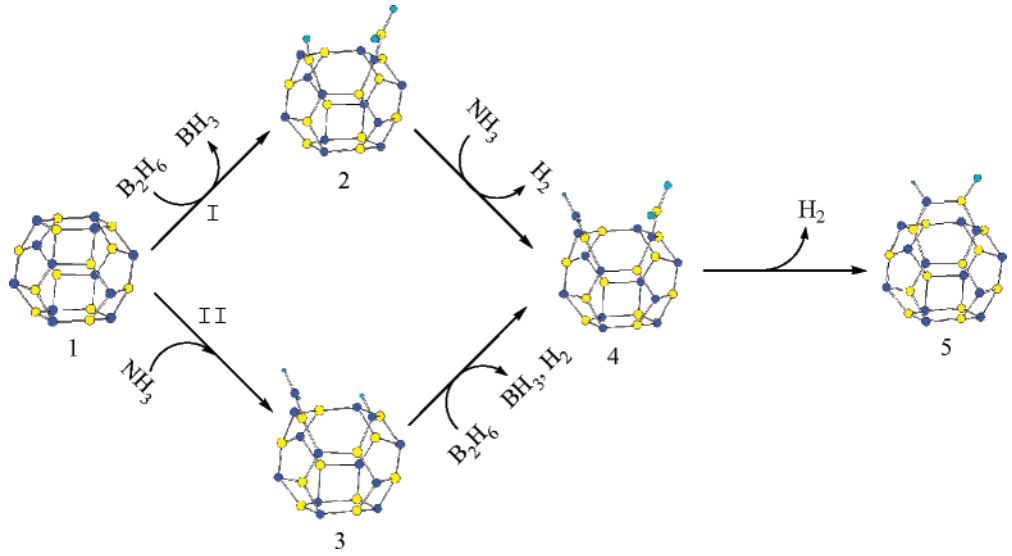

SCHEME 3. Growth of the Armchair (3,3) Tube

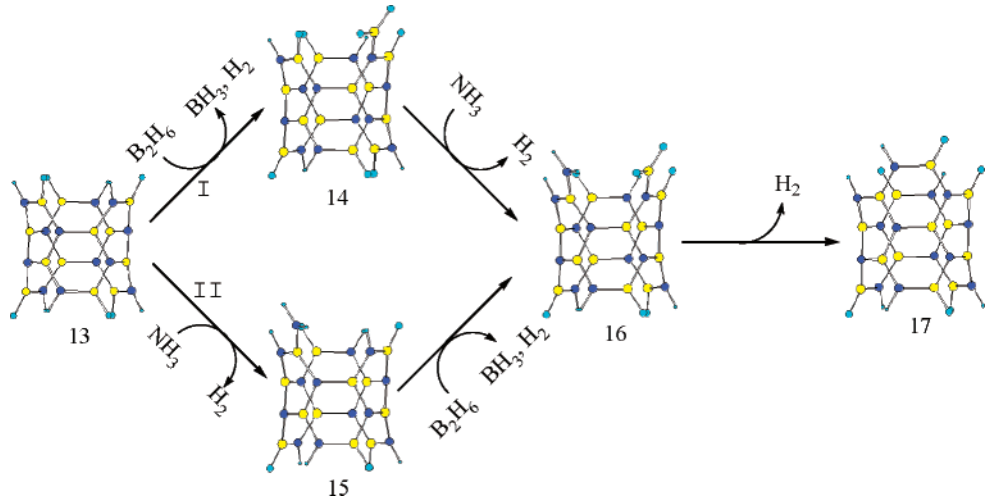

B_2H_6, one of reactants, has a hydrogen-bridged structure[21,22] with the terminal and bridged B−H bond lengths of 1.180 and 1.318 Å (at the level of HF/6-31G), respectively. So, the bridged B−H bonds are so weak that they are easily broken at the proposed experimental conditions such as high temperature. The optimized structures at the HF/6-31G level of reactant **1**, intermediates **2**−**7**, transition states **8**−**12TS**, and products along two pathways are collected in Figure 2 with some important bond lengths and charges (in parentheses) shown in it. The relative electronic energies ΔE (in kcal/mol) of intermediates, transition states, and products to the reactant calculated by MP2 method with the 6-31G basis set are listed in Table 3. Accordingly, potential energy profiles for two paths are depicted in Figure 3.

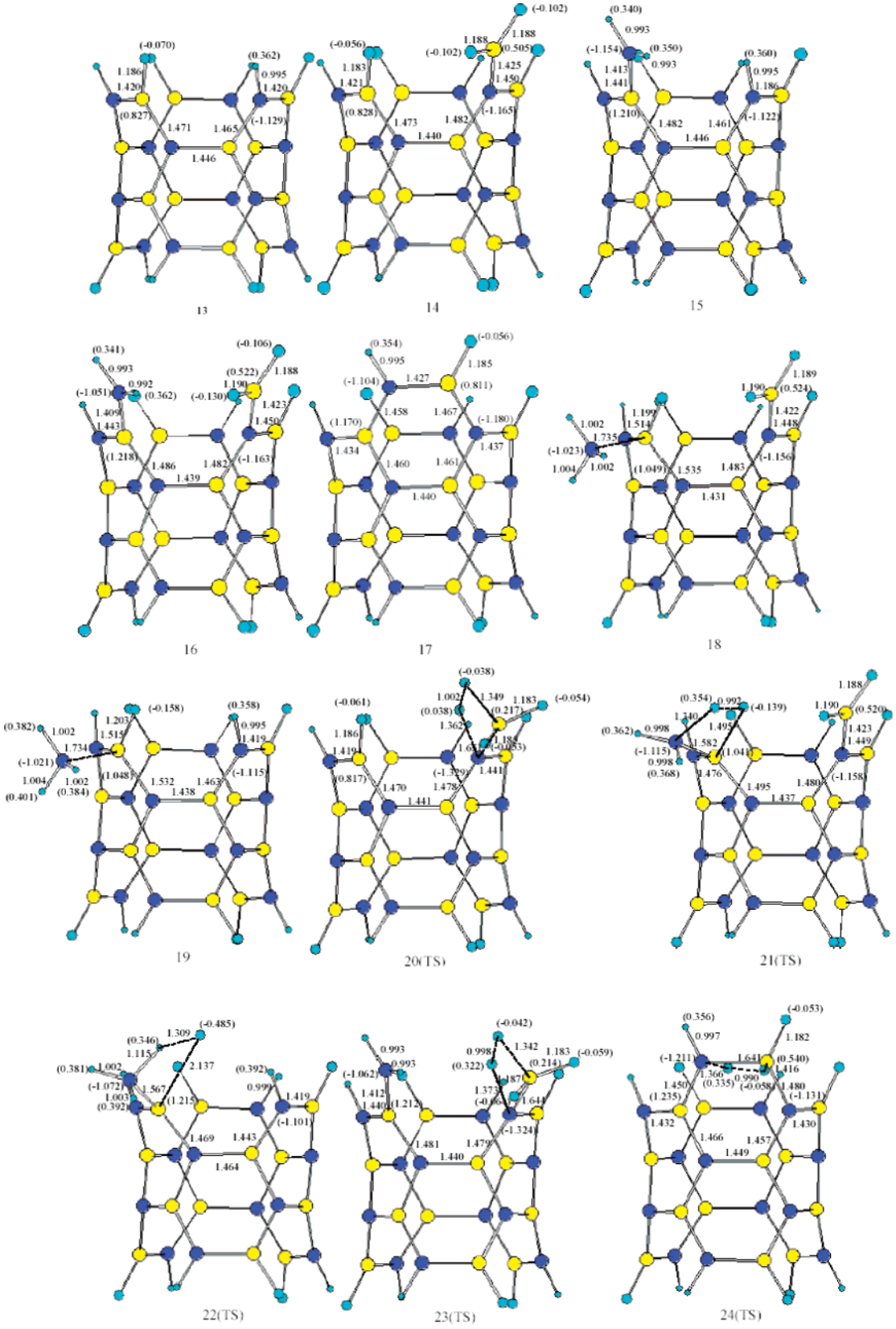

Figure 4. The optimized structures of reactants, intermediates, transition states, and products for the growth of the armchair (3,3) tube at the HF/6-31G level.

From Figure 3 and Table 3, we can clearly see that in the pathway I, the square of $B_{12}N_{12}$ fullerene (**1**) can be easily opened by B_2H_6 via a transition state **8TS**. The activation barrier for this process is only 13.53 kcal/mol, and the resulting intermediate **2** is 22.36 kcal/mol below the reactant **1**. Then **2** reacts with NH_3 to form an intermediate **6**, liberating the association energy of 38.61 kcal/mol. The further reaction of **6** with NH_3 through **9TS** has a high activation barrier of 58.91 kcal/mol and arrives intermediate **4**, which is only 0.37 kcal/mol above **6**. The formation of a new hexagon in product **5** requires **4** to further dissociate a H_2 molecule by overcoming a large barrier of 57.57 kcal/mol via **12TS**. So, the reaction of **6**

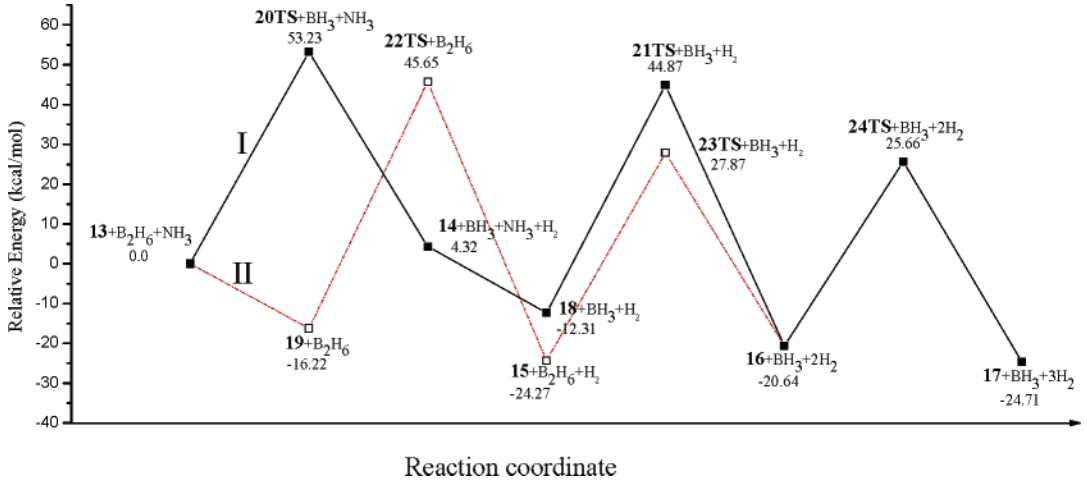

Figure 5. Potential energy profiles for the growth of the armchair (3,3) tube.

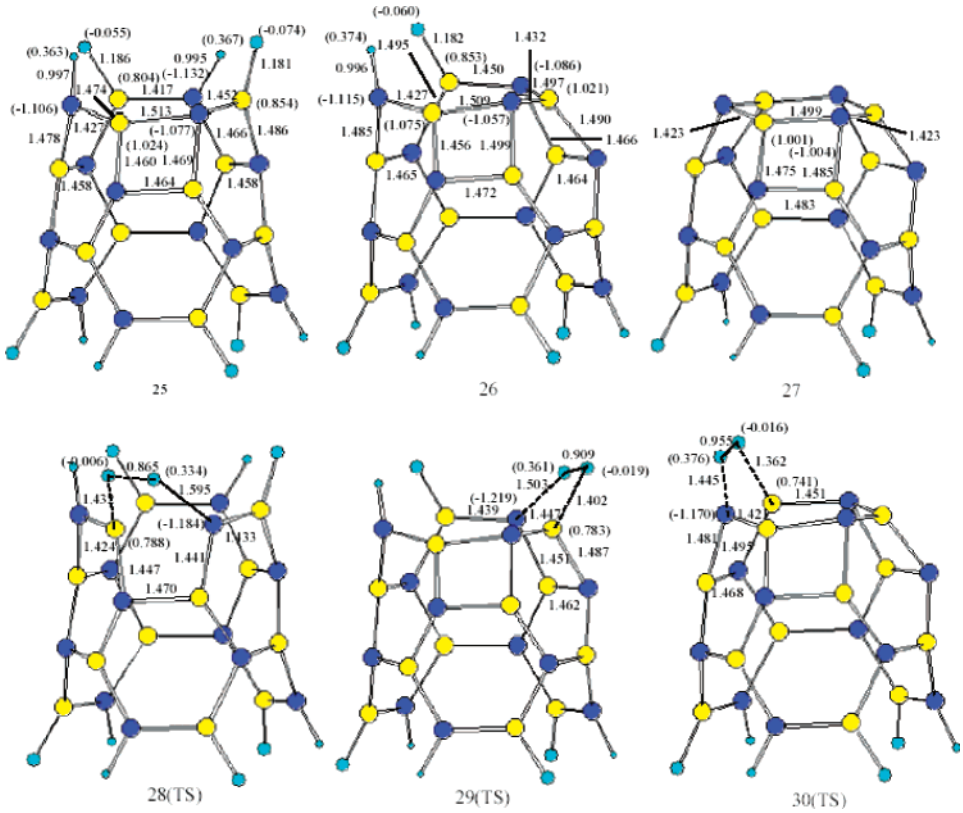

Figure 6. The optimized structures of intermediates and transition states for the capping of the armchair (3,3) tube at the HF/6-31G level.

SCHEME 4. Capping of the Armchair (3,3) Tube

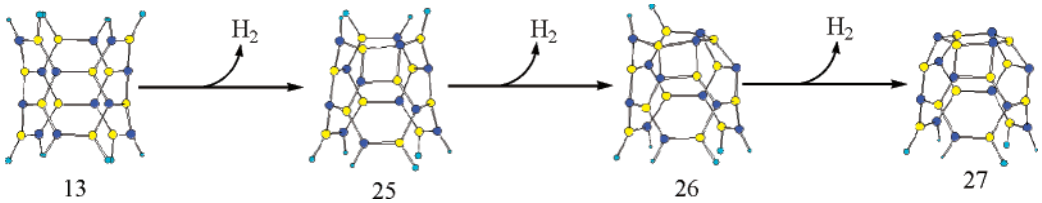

with NH_3 and the formation of a hexagon from **4** are the rate-limiting steps. In pathway II, **1** can react with NH_3 to form a fullerene−NH_3 complex **7** via a barrierless process, which is exothermic by 47.71 kcal/mol. Then the intermediate **7** opens its square through **10TS** to form **3**. The activation barrier for this process is 28.86 kcal/mol, and this step is exothermic by 13.68 kcal/mol. The further reaction of the intermediate **3** with B_2H_6 via **11TS** has a barrier of 50.62 kcal/mol, leading to **4** from which the same process to form a hexagon in **5** as in path I are followed. So, it is possible for a $B_{12}N_{12}$ fullerene (**1**) to react with B_2H_6 and NH_3 to form an armchair (3,3) tubular structure under a condition of the high temperature. Furthermore, the square in the $B_{12}N_{12}$ fullerene is relatively more readily opened by NH_3 than B_2H_6 because the process of NH_3 reacting with $B_{12}N_{12}$ fullerene to form a stable $B_{12}N_{12}$−NH_3 intermediate liberates a large association energy of 47.71 kcal/mol, which is

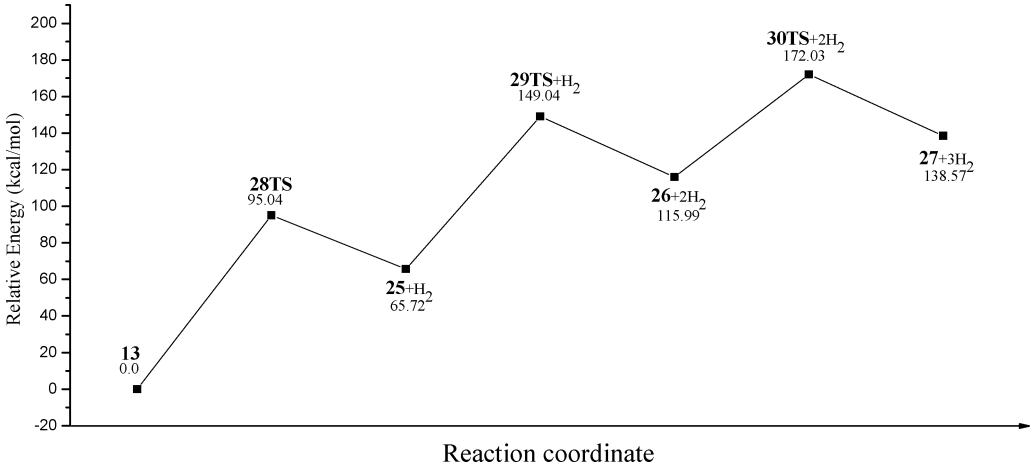

Figure 7. Potential energy profile for the capping of the armchair (3,3) tube.

SCHEME 5. Decapping of the Closed Armchair (3,3) Tube

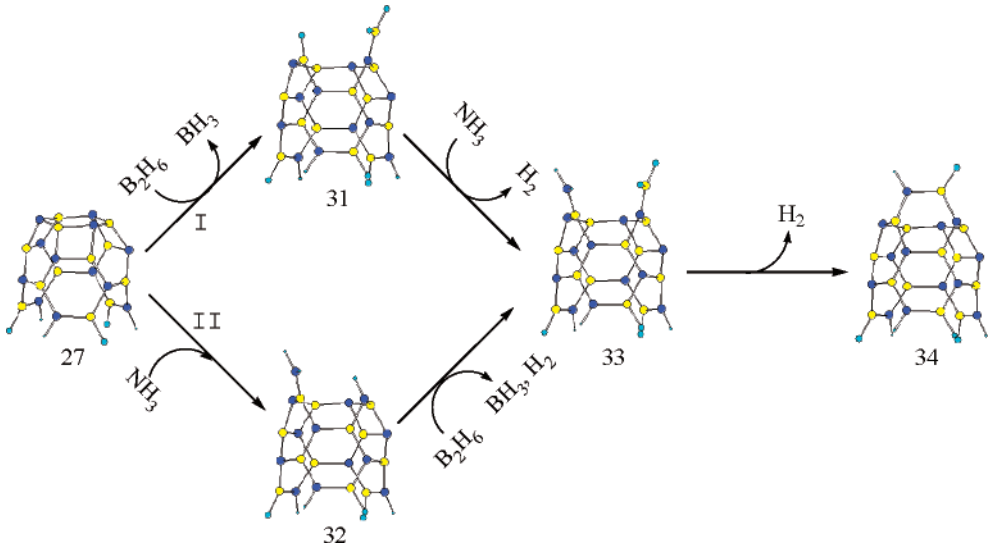

TABLE 3: Relative Electronic Energies, ΔE, of Reactants, Intermediates, Transition States, and Products along Two Pathways of the Formation of the Armchair (3,3) Tubular Structures (MP2/6-31G//HF/6-31G)

species	ΔE (kcal/mol)
1 + B_2H_6 + NH_3	0.0
2 + BH_3 + NH_3	−22.36
3 + B_2H_6	−61.39
4 + BH_3 + H_2	−60.60
5 + BH_3 + $2H_2$	−50.01
6 + BH_3	−60.97
7 + B_2H_6	−47.71
8TS + BH_3 + NH_3	13.53
9TS + BH_3	−2.06
10TS + B_2H_6	−18.85
11TS + BH_3	−10.77
12TS + BH_3 + H_2	−3.03

adequate for counteracting the required activation energy (28.86 kcal/mol) in the following open-ring reaction. But, the barriers of the rate-limiting steps of two paths are very close to each other, thus both pathways are possible to take place under the same condition.

The Growth of the Armchair (3,3) Tube. The armchair (3,3) tube keeps growing when it continuously incorporates B and N atoms from reactants B_2H_6 and NH_3. We have studied the growth mechanism of the armchair (3,3) tube in the B_2H_6 and NH_3 atmosphere. Two possible pathways (Scheme 3) are considered: (I) the armchair (3,3) tube (**13**) is first attacked by the B_2H_6 and then the NH_3 molecules to form a hexagon in **16** and (II) molecule **13** incorporates a N atom first and then a B atom, yielding intermediates **15** and **16**, respectively.

The optimized structures at the HF/6-31G level of reactant **13**, intermediates **14**−**19**, and transition states **20**−**24TS** along two pathways are given in Figure 4. The potential energy profiles of both paths during this process are plotted in Figure 5 with their relative electronic energies ΔE (in kcal/mol) to **13** at the MP2/6-31G level listed in Table 4.

It can be seen from Figure 5 that, in pathway I, the reaction for the armchair (3,3) tube **13** to incorporate a B atom from B_2H_6 has a barrier of 53.23 kcal/mol, and form an intermediate **14**, which is 4.32 kcal/mol above the reactant **13**. Then **14** further reacts with the NH_3 to form an intermediate **18**, releasing an association energy of 16.63 kcal/mol. The activation barrier for further dissociating a H_2 molecule from **18** through **21TS** to another intermediate **16** is 57.18 kcal/mol. The formation of a new hexagon in **17** needs the dissociation of another H_2 molecule from **16** with a barrier of 46.30 kcal/mol. Pathway II only differs from path I in the first two steps. Reactant **13** with tubular structure first reacts with NH_3 to form intermediate **19** with the association energy of 16.22 kcal/mol in path II. Then the barrier for releasing a H_2 molecule from **19** to yield another intermediate **15** via **22TS** is 61.87 kcal/mol with the process being exothermic by 8.05 kcal/mol. And the barrier for **15** to further incorporate a B atom from B_2H_6 through **23TS** is 52.14

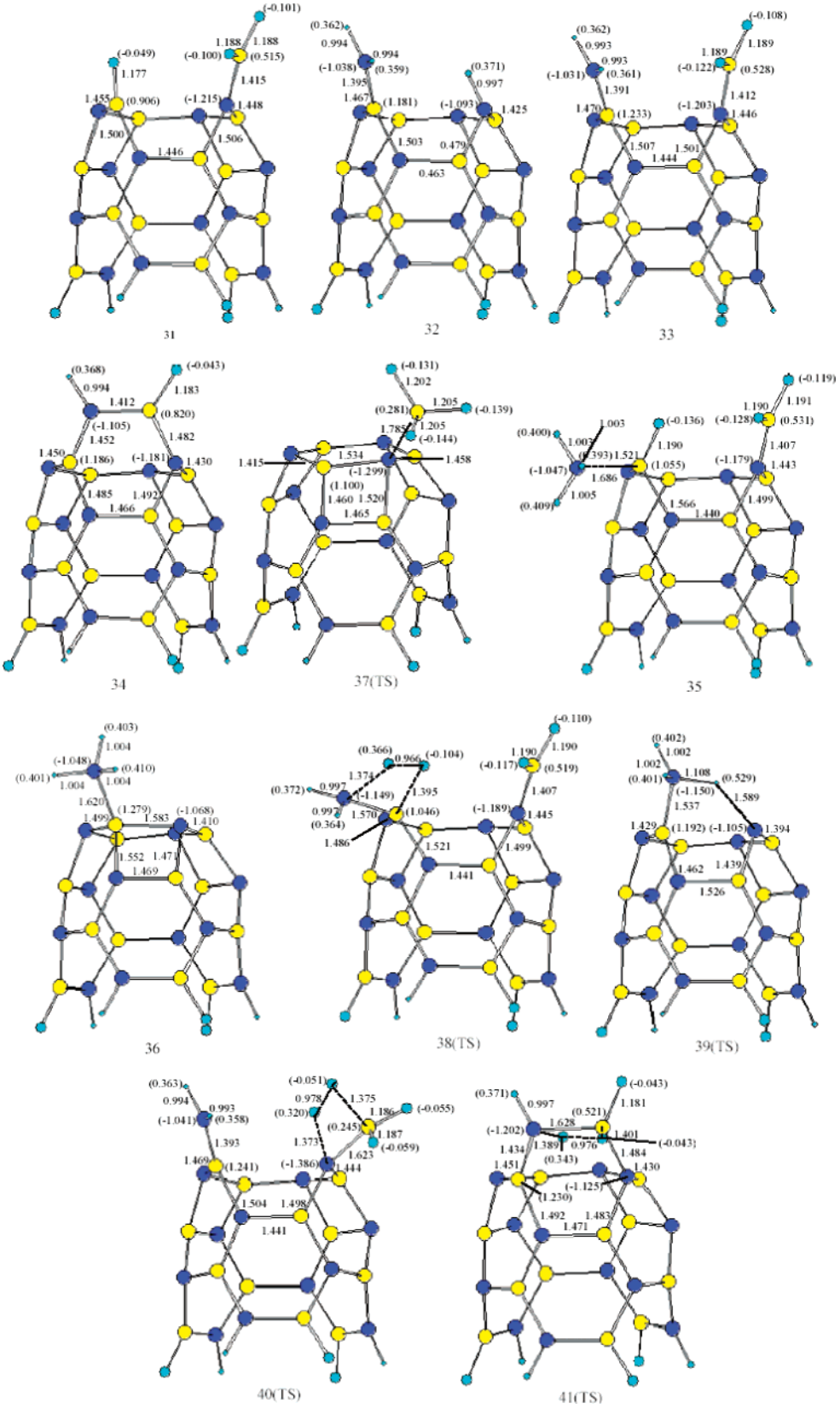

Figure 8. The optimized structures at the HF/6-31G level of reactants, intermediates, and transition states for the decapping of the one close-ended armchair (3,3) tube.

kcal/mol, giving rise to the intermediate **16**. After that, the same reaction process as in path I from **16** to **17** takes place. In summary, the reaction of the open-ended armchair (3,3) tube **13** with B_2H_6 has an activation barrier of about 52−53 kcal/mol, and the reaction of the armchair (3,3) tube with NH_3 first undergoes a barrierless process to yield the association energy of around 16 kcal/mol and subsequently climbs over a barrier of about 57−62 kcal/mol. The formation of a new hexagon has a barrier of 46.30 kcal/mol.

The Capping and Decapping of the Armchair (3,3) Tube. In the experimental condition, there also exists a possibility for the formed BN tube to be closed into a cap, which may prevent

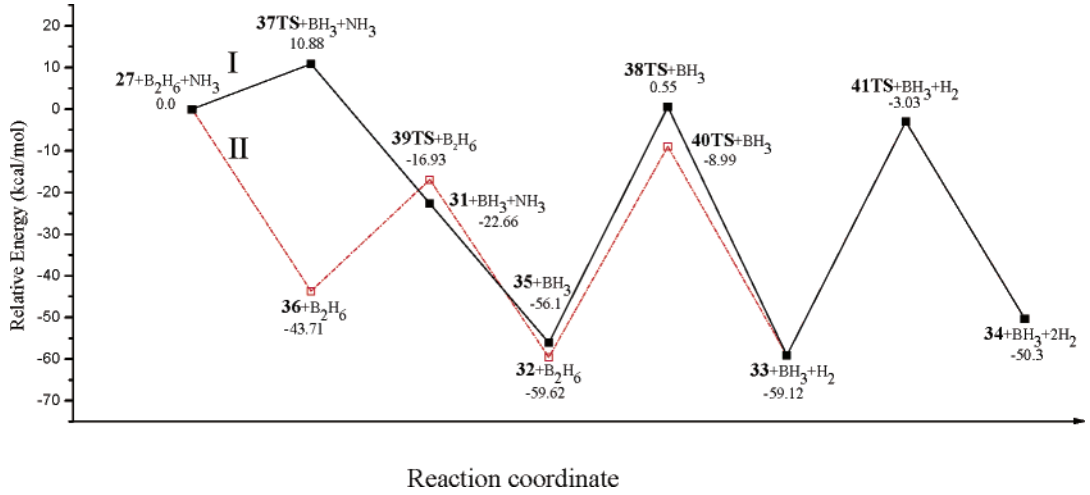

Figure 9. Potential energy profile for the capping of the one close-ended armchair (3,3) tube.

TABLE 4: Relative Electronic Energies Δ*E* of Reactants, Intermediates, Transition States, and Products along Two Pathways of the Growth of the Armchair (3,3) Tube (MP2/6-31G//HF/6-31G)

species	Δ*E* (kcal/mol)
13 + B_2H_6 + NH_3	0.0
14 + BH_3 + NH_3 + H_2	4.32
15 + B_2H_6 + H_2	−24.27
16 + BH_3 + $2H_2$	−20.64
17 + BH_3 + $3H_2$	−24.71
18 + BH_3 + H_2	−12.31
19 + B_2H_6	−16.22
20TS + BH_3 + NH_3	53.23
21TS + BH_3 + H_2	44.87
22TS + B_2H_6	45.65
23TS + BH_3 + H_2	27.87
24TS + BH_3 + $2H_2$	25.66

TABLE 5: Relative Electronic Energies, Δ*E*, of Intermediates and Transition States of the Capping of the Armchair (3,3) Tube (MP2/6-31G//HF/6-31G)

species	Δ*E* (kcal/mol)
13	0.0
25 + H_2	65.72
26 + $2H_2$	115.99
27 + $3H_2$	138.57
28TS	95.04
29TS + H_2	149.04
30TS + $2H_2$	172.03

the further growth of the tube.[23−25] Here, we study the possible mechanisms of a formation of a half-$B_{12}N_{12}$ cap at the top of the armchair (3,3) tube by dissociating three H_2 molecules and of the opposite decapping process to form an open-ended tubular structure for further growth.

Scheme 4 describes a possible capping process of successive dissociation of 3 H_2 molecules from the armchair (3,3) tube to form three squares and close into a half-$B_{12}N_{12}$ cap. Its reverse reaction is the association reactions with H_2 to open the tube's cap. The optimized structures at the HF/6-31G level of all intermediates **25**−**27** and transition states **28**−**30TS** along the capping process are displayed in Figure 6 with their relative electronic energies Δ*E* (in kcal/mol, calculated by MP2/6-31G) listed in Table 5. Accordingly, the potential energy profile for this process is plotted in Figure 7. The successive dissociations of H_2 molecules from the armchair tube **13** to close into a half-$B_{12}N_{12}$ cap (i.e., steps of **13**−**25**, **25**−**26**, and **26**−**27**) have extremely high barriers of 95.04, 83.32, and 56.04 kcal/mol, respectively (cf. Figure 7 and Table 5). And the close-ended tube is much less stable than the open-ended tube. In contrast, the reverse reactions, associations of H_2 to the closed tube, have smaller barriers of 33.46, 30.05, and 29.32 kcal/mol. So in the atmosphere of H_2, it is difficult for the armchair (3,3) tube to be closed into a half-$B_{12}N_{12}$ cap.

TABLE 6: Relative Electronic Energies, Δ*E*, of Reactants, Intermediates, and Transition States along Two Pathways of the Decapping of the One Close-Ended Armchair (3,3) Tube (MP2/6-31G//HF/6-31G)

species	Δ*E* (kcal/mol)
27 + B_2H_6 + NH_3	0.0
31 + BH_3 + NH_3	−22.66
32 + B_2H_6	−59.62
33 + BH_3 + H_2	−59.12
34 + BH_3 + $2H_2$	−50.30
35 + BH_3	−56.10
36 + B_2H_6	−43.71
37TS + BH_3 + NH_3	10.88
38TS + BH_3	0.55
39TS + B_2H_6	−16.93
40TS + BH_3	−8.99
41TS + BH_3 + H_2	−3.03

The closed armchair (3,3) tube can also be decapped by B_2H_6 and NH_3: the half-$B_{12}N_{12}$ cap can incorporate B and N atoms and revert to a growing open-ended tubular structure (Scheme 5). There are two possible pathways of the decapping process: (I) the one close-ended armchair (3,3) tube, **27**, incorporates a B atom from B_2H_6 to open a square and then incorporates a N atom from NH_3 to form a hexagon and (II) **27** with a half-$B_{12}N_{12}$ cap is first opened by NH_3 and then by B_2H_6 to form a hexagon. Figure 8 gives the optimized structures at the HF/6-31G level of reactant **27**, intermediates **31**−**36**, and transition states **37**−**41TS** along these two pathways with their relative electronic energies Δ*E* (in kcal/mol) calculated by MP2/6-31G presented in Table 6. The potential energy profiles for those processes are shown in Figure 9.

The reaction mechanisms of the half-$B_{12}N_{12}$ capped tube (**27**) with B_2H_6 and NH_3 as shown in Figure 9 are very similar to those of the reaction of the $B_{12}N_{12}$ fullerene (**1**) with B_2H_6 and NH_3 (cf. Figure 3). The decapping processes have close activation barriers to the formation reaction of the tube from fullerene **1**. In pathway I, the square of the half-$B_{12}N_{12}$ cap can be easily opened by B_2H_6 with a small barrier of 10.88 kcal/mol. The resulting intermediate **31** is 22.66 kcal/mol below the reactant **27**. After the cap's square is opened, the further reaction with NH_3 has a greater barrier of 56.65 kcal/mol. In pathway II, the cap in **27** reacts with NH_3 to form an intermediate **36** by

releasing the association energy of 43.71 kcal/mol. The barrier for **36** to open its square is only 26.78 kcal/mol. Once the square in the cap is opened by NH_3, the further reaction with B_2H_6 needs to overcome a barrier of 50.63 kcal/mol. The final steps in both pathways are the same: a new hexagon is formed from intermediate **33** through **41TS** with a barrier of 56.09 kcal/mol. Similar to the formation process of the tube, the rate-limiting steps of both decapping paths have comparable activation barriers. It suggests that both the pathways are possible to take place at high temperature. Therefore, the one close-ended armchair (3,3) tube may be decapped by B_2H_6 and NH_3 and reverted to a growing open-ended tubular structure under certain experimental conditions.

4. Conclusion

The electronic structures and formation mechanisms of the armchair (3,3) BN tube have been investigated by theoretical calculations. The armchair (3,3) BN tube has a very close thermodynamic stability to and greater kinetic stability than the observed zigzag (6,0) BN tube (in E. Bengu's experiment),[15] revealing a possibility of producing the armchair (3,3) tube.

The armchair (3,3) tube is shown to share similarities with fullerene $B_{12}N_{12}$ such as the comparable radii and stability. Thus, $B_{12}N_{12}$ is selected as a model starting reactant to study the mechanisms of formation and growth processes of an armchair (3,3) tubular structure. Our calculations show that a $B_{12}N_{12}$ fullerene, which has been observed in experiments,[13,14] can react with B_2H_6 and NH_3 to form an armchair (3,3) tubular structure under certain conditions such as high temperature. The square of a $B_{12}N_{12}$ fullerene can be opened by B_2H_6 and NH_3 with barriers of 13.53 and 28.86 kcal/mol, respectively. After that, reactions along different paths go into the rate-limiting steps of building a new hexagon to form an armchair (3,3) tubular structure, which have barriers of around 50−60 kcal/mol.

The open-ended armchair (3,3) tube can react continuously with B_2H_6 and NH_3 to form a new hexagon network and keep growing. The reaction of the open-ended armchair (3,3) tube with B_2H_6 has the activation barrier of about 52−53 kcal/mol, and the reaction of the tube with NH_3 has the barrier of 57−62 kcal/mol. Finally, the formation of a new hexagon has a barrier of 46.30 kcal/mol.

There may exist a competitive process for the growth of the BN tube; i.e., the open-ended armchair (3,3) tube dissociates three H_2 molecules and closes into a half-$B_{12}N_{12}$ cap. But the capping processes are demonstrated to have much greater barriers (around 95.04 kcal/mol) than those of the growth of the open-ended tube in the B_2H_6 and NH_3 atmosphere (around 50−60 kcal/mol). So in the B_2H_6 and NH_3 atmosphere, the growth of the tube is favorable. If the tube is closed during the capping process, our calculations also indicate that H_2, B_2H_6, and NH_3 can open the tube cap and convert the tube to a growing open-ended structure. So the armchair (3,3) tube can keep growing under certain conditions.

In summary, we can expect that someday in the future the armchair (3,3) BN tube can be also observed like those of $B_{12}N_{12}$ and $B_{16}N_{16}$ fullerenes[13,14] and the zigzag (6,0) tube.[15]

Acknowledgment. This work was financially supported by Natural Science Foundations of China (Nos. 20103004, 90303020, and 10175034), the National Key Project for High-Tech (No. 2003AA302150), as well as the High-Tech Project of Jiangsu Province (BG2003029).

References and Notes

(1) Baughman, R. H.; Zakhidov, A. A.; De Heer W. A. *Science* **2002**, *297*, 787.
(2) Collins, P. G.; Zettl, A.; Bando, H.; Thess, A.; Smalley, R. E. *Science* **1997**, *278*, 100.
(3) Ajayan, P. M., Iijima, S. *Nature* **1992**, *358*, 23.
(4) Sun, L. F.; Xie, S. S.; Liu, W.; Zhou, W. Y.; Liu, Z. Q.; Tang, D. S.; Wang, G.; Qian, L. X. *Nature* **2000**, *403*, 384.
(5) Qin, L. C.; Zhao, X. L.; Hirahara, K.; Miyamoto, Y.; Ando, Y.; Iijima, S. *Nature* **2000**, *408*, 50.
(6) Wang, N.; Tang, Z. K.; Li, G. D.; Chen, J. S. *Nature* **2000**, *408*, 50.
(7) Peng, H. Y.; Wang, N.; Zheng, Y. F.; Lifshitz, Y.; Kulik, J.; Zhang, R. Q.; Lee, C. S.; Lee, S. T. *Appl. Phys. Lett.* **2000**, *77*, 2831.
(8) Blase, X.; Rubio, A.; Louie, S. G.; Cohen, M. L. *Europhys. Lett.* **1994**, *28*, 335.
(9) Jensen, F.; Toftlund, H. *Chem. Phys. Lett.* **1993**, *201*, 89.
(10) Fowler, P. W.; Heine, T.; Mitchell, D.; Schmidt, R.; Seifert, G. *J. Chem. Soc., Faraday Trans.* **1996**, *92*, 2197.
(11) Sun, M. L.; Slanina, Z.; Lee S. L. *Chem. Phys. Lett.* **1995**, *233*, 279.
(12) Seifert, G.; Fowler, P. W.; Mitchell, D.; Frauenheim T. *Chem. Phys. Lett.* **1997**, *268*, 352.
(13) Loiseau, A.; Willaime, F.; Demoncy, N.; Schramchenko, N.; Hug, G.; Colliex, C.; Pascard, H. *Carbon* **1998**, *36*, 743.
(14) Stéphan, O.; Bando, Y.; Loiseau, A.; Willaime, F.; Schramchenko, N.; Tamiya, T.; Sato, T. *Appl. Phys. A* **1998**, *67*, 107.
(15) Bengu, E.; Marks, L. D. *Phys. Rev. Lett.* **2001**, *86*, 2385.
(16) Tang, Z. K.; Zhang, L. Y.; Wang, N.; Zhang, X. X.; Wen, G. H.; Li, G. D.; Wang, J. N.; Chan, C. T.; Sheng, P. *Science* **2001**, *292*, 2462.
(17) Frisch, M. J.; Trucks, G. W.; Schlegel, H. B.; Scuseria, G. E.; Robb, M. A.; Cheeseman, J. R.; Zakrzewski, V. G.; Montgomery, J. A., Jr.; Stratmann, R. E.; Burant, J. C.; Dapprich, S.; Millam, J. M.; Daniels, A. D.; Kudin, K. N.; Strain, M. C.; Farkas, O.; Tomasi, J.; Barone, V.; Cossi, M.; Cammi, R.; Mennucci, B.; Pomelli, C.; Adamo, C.; Clifford, S.; Ochterski, J.; Petersson, G. A.; Ayala, P. Y.; Cui, Q.; Morokuma, K.; Malick, D. K.; Rabuck, A. D.; Raghavachari, K.; Foresman, J. B.; Cioslowski, J.; Ortiz, J. V.; Stefanov, B. B.; Liu, G.; Liashenko, A.; Piskorz, P.; Komaromi, I.; Gomperts, R.; Martin, R. L.; Fox, D. J.; Keith, T.; Al-Laham, M. A.; Peng, C. Y.; Nanayakkara, A.; Gonzalez, C.; Challacombe, M.; Gill, P. M. W.; Johnson, B. G.; Chen, W.; Wong, M. W.; Andres, J. L.; Head-Gordon, M.; Replogle, E. S.; Pople, J. A. *Gaussian 98*, revision A.11; Gaussian, Inc.: Pittsburgh, PA, 1998.
(18) Zhang, R. Q.; Chu, T. S.; Lee, S. T. *J. Chem. Phys.* **2001**, *114*, 5531.
(19) Zhang, D.; Zhang, R. Q. *Chem. Phys. Lett.* **2003**, *371*, 426.
(20) Pokropivny, V. V.; Skorokhod, V. V.; Oleinik, G. G.; Kurdyumov, A. V.; Bartnitskaya, T. S.; Pokropivny, A. V.; Sisonyuk, A. G.; Sheichenko, D. M. *J. Solid State Chem.* **2000**, *154*, 214.
(21) Page, M.; Adams, G. F.; Binkley, J. S.; Melius, C. F. *J. Phys. Chem.* **1987**, *91*, 2675.
(22) Curtiss, L. A.; Pople J. A. *J. Chem. Phys.* **1988**, *89*, 4875.
(23) Menon, M.; Srivastava, D. *Chem. Phys. Lett.* **1999**, *307*, 407.
(24) Charlier, J. C.; Blase, X.; Vita, A. D.; Car, R. *Appl. Phys. A* **1999**, *68*, 267.
(25) Blase, X.; Vita, A. D.; Charlier, J. C.; Car, R. *Phys. Rev. Lett.* **1998**, *80*, 1666.